Silica-rich septarian concretions in biogenic silica-poor sediments: A marker of hydrothermal activity at fossil hyper-extended rifted margins (Err nappe, Switzerland)

SILICA-RICH SEPTARIAN CONCRETIONS IN BIOGENIC SILICA-POOR SEDIMENTS: A MARKER OF HYDROTHERMAL ACTIVITY AT FOSSIL HYPER-EXTENDED RIFTED MARGINS (ERR NAPPE, SWITZERLAND).

NICOLÒ INCERPI[1*], LUCA MARTIRE[2], STEFANO M. BERNASCONI[3], GIANRETO MANATSCHAL[1] AND AXEL GERDES[4]

[1]*Institut de Physique du Globe de Strasbourg, CNRS-UMR 7516, EOST, Université de Strasbourg, 1 rue du Blessig, 67084 Strasbourg, France.* nincerpi@unistra.fr tel +33 368850418 fax +33 368850402*;* manat@unistra.fr tel +33 368850454 fax +33 368850402

[2]*Dipartimento di Scienze della Terra, Università degli Studi di Torino, Via Valperga Caluso 35, 10125 Torino, Italy;* luca.martire@unito.it, tel +39 0116705194 fax +39 0116705339

[3]*Geological Institute, ETH Zürich, Sonneggstrasse 5, 8092 Zürich, Switzerland;* stefano.bernasconi@erdw.ethz.ch tel +41 446323693 fax +41 446327543

[4] *Institute of Geosciences, Goethe University of Frankfurt, Altenhöferallee 1, 60438 Frankfurt am Main, Germany* gerdes@em.uni-frankfurt.de tel +49 069 798 40152

Corresponding author: Nicolò Incerpi nincerpi@unistra.fr

ABSTRACT

Silica-rich septarian concretions occur within Pliensbachian-Oxfordian syn-rift to early post-rift sediments of the fossil distal Adriatic rifted margin today exposed in the Err nappe (Central Alps). The concretions, ranging in size from few centimeters to about 2 meters, consist of partially to completely siliceous spheroidal bodies developed within fine-grained sedimentary rock (mud to fine sand) with no or very scarce content in biogenic silica such as radiolarian tests. These concretions are characterized by a network of septarian cracks filled with chalcedony, quartz and locally, saddle dolomite. Some concretions are in their original position, whereas others are fragmentary and preserved in coarse-grained turbiditic beds, implying that concretionary growth had occurred prior to significant burial. Fluid inclusion temperatures (~150°C), the positive $\delta^{18}O$ values for original fluids (up to +7‰ SMOW), and the high $^{87}Sr/^{86}Sr$ values of dolomite point to a deep circulation of seawater into fault damage zones developed in granitic basement rocks. In their ascent, these hot, silica-rich fluids crossed compact sediments giving rise to quartz-dolomite veins. Lastly, when reaching the uncompacted soft sediments close to the seafloor, silica (quartz and chalcedony) locally precipitated in sediment pores and/or fissures leading to the formation of the siliceous septarian concretions. The anomalous quartz-rich mineralogy of the concretion body and of the authigenic crack-filling minerals, the occurrence in clastic sediments from deep-water distal rifted margins as well as high formation temperatures represent a new discovery enlarging the spectrum of septarian concretion types and the environment where they may grow. They provide a possible record of the subbottom products of hydrothermal venting typifying hyper-extended rifted margins where extensional detachment faults exhume crustal rocks to the seafloor and lead to an intense fluid-rock interaction and silica enrichment in the fluids.

Keywords: silica-rich septarian concretions, hydrothermal fluids, hyper-extended rifted margin, Err nappe

1. INTRODUCTION

Septarian concretions, that commonly occur within mudstone dominated successions, are characterized in their interior by cracks partially to completely filled with authigenic minerals. These cracks, often polyphase, are mainly radial and reach the greatest width at the center of the concretion and wedge out at its periphery. Concentric cracks also occur. Several hypotheses have been put forward to explain their origin. These include: fluid overpressure during burial (e.g. barrett and Scotchman, 1988; Selles-Martinez, 1996, 1998), stress release due to erosion (Hounslow, 1997), seismic shocks (Pratt, 2001), and syneresis associated with degradation of extracellular polymeric substances (Hendry et al. 2006). Concretion bodies are usually cemented by carbonates, whereas septarian cracks may be lined by carbonates or pyrite. Silica-rich concretions with septarian-like cracks have been reported in the literature even if they are much less common and strictly related to particular settings such as: 1) Precambrian iron-rich formations affected by syneresis interpreted to be due to dewatering of silica gels (e.g. Gross, 1972), 2) continental environments where desiccation processes or magadiite-quartz transformation have been suggested (e.g. Schubel and Simonson 1990), or 3) diatom-rich sediments where siliceous spheroidal concretions with concentric cracks were interpreted due to differential compaction between early lithified concretions and the unlithified highly porous host sediments (Behl, 2011).

Siliceous septarian concretions have been recently found in the Middle Jurassic succession deposited in the most distal and hyperextended parts of the Tethyan Adriatic margin, preserved

in the Austroalpine Err Nappe in SE Switzerland (Incerpi, 2017; Incerpi et al., 2017; Figs. 1A-B-C). They differ from usual septarian concretions because of the composition of the cementing mineral, which is microquartz instead of the overwhelmingly more common carbonates (e.g. Pratt, 2001), and from normal chert nodules, commonly found in pelagic, biogenic opal-rich sediments, for the occurrence of septarian-like cracks filled with quartz or chalcedony. Furthermore, they occur in a context in which hydrothermal processes are recorded. As documented by Incerpi et al. (2017), the distal Adriatic rifted margin experienced a multi-stage, rift-related fluid evolution affecting the pre- to early post--rift sediments of Triassic to early Late Jurassic age. The connection between hyper-extension and hydrothermal fluid flow is becoming essential in the prediction of the thermal state and the evolution of distal rifted margins and its influence on critical parameters such as permeability, porosity and heat fluxes in sedimentary basins as well as for the diagenetic evolution of the associated sediments (Pinto et al., 2015). This study presents a large dataset resulting from a multidisciplinary analysis including stratigraphic relationships, petrography, isotope (C, O, Sr) geochemistry, and fluid inclusion microthermometry. It aims to report a new, previously undescribed hydrothermal-related silica-rich type of septarian concretions, which provides strong evidence for hot fluid flow in shallowly buried soft sediments deposited at deep-water hyperextended rifted margins. It is worth clarifying that, as proposed by previous authors (e.g. Selles-Martinez, 1996; Mozley, 2003) the term concretion is here meant as a portion of a sedimentary rock which has been cemented differentially from its host.

2. GEOLOGICAL SETTING

The distal Adriatic rifted margin (Fig. 1C) formed after a phase of distributed rifting, during Pliensbachian to Callovian, leading to the opening of the Alpine Tethys ocean (Mohn et al., 2011). This evolution is characterized by the transition from high-angle normal faults to extensional detachment faults dissecting pre-rift Paleozoic basement (mainly granites in the study area) and pre-rift sediments (Upper Triassic-Lower Jurassic dolostones and limestones). This process led to the creation of a rugged morphology dominated by extensional allochthons made of pre-rift rocks bounding supra-detachment sedimentary basins floored by detachment faults (Masini et al. 2011). These starved basins were filled by no more than few hundreds of meters thick syn-rift sediments that range from tectono-sedimentary breccias at the base to debris flows and turbidites interbedded with fine-grained sediments further upsection (Bardella and Saluver Formations, Masini et al. 2011). Both the extensional allochthons and the syn-rift sedimentary basins are sealed by the post-rift Callovian-Oxfordian Radiolarian Cherts representing the first sediments occurring over pillow basalts in the adjacent exhumed mantle domain (Weissert and Bernoulli, 1985; Wilson et al., 2001). The pre-rift sedimentary sequence in the Err nappe is composed of Ladinian to Norian platform carbonates (Hauptdolomit Fm.), Rhaetian limestones and shales (Kössen Fms.) and Lower Jurassic sponge spicule-bearing cherty limestones alternated with marls (Agnelli Fm.).

The syn-rift sediments consist of complex gravitational to hemipelagic sedimentary deposits that occur either unconformably over extensional allochthons or directly over the tectonically exhumed basement. Finger (1978) distinguished these syn-rift sediments in two formations, the Bardella and Saluver Fms. The subdivision is based on their composition: the Bardella Fm. is made of clast-supported breccias with clasts of Triassic to Early Jurassic carbonates whereas the Saluver Fm., still being a coarse sedimentary breccia, includes mainly basement-derived

material. Finger (1978) further subdivided the Saluver Fm. into a coarse-grained, poorly organised Saluver A sub-formation at the base, an intermediate Saluver B made of polimict breccias and litharenites showing a thinning- and fining-upward trend from clast-supported breccias to turbidites. Lastly, the top member (Saluver C) corresponds to black shales interbedded with thin distal turbidites with subordinate conglomerates and mature arkosic beds. A progressive fining upward trend leads to the overlying post-rift Radiolarian Chert Fm. The thickness of the syn-rift sediments along the margin is highly variable ranging from some hundreds of meters to only few tens of meters.

Several papers (Manatschal, 1999; Manatschal et al., 2000; Pinto et al.,2015; Incerpi et al., 2017) showed that the evolution of the Adriatic distal margin is intimately connected with a complex fluid flow history affecting both basement rocks and pre- to post-rift sediments. Incerpi et al. (2017) demonstrated that this complex fluid history is at the origin of several different hydrothermal products (e.g. clay-rich gouges, quartz veins, chloritization of feldspars in the tectonized granites; replacement minerals, hydrothermal breccias, veins) developed diachronously along the evolution of the margin. One of the most outstanding fluid-related products detected in the distal Adriatic margin are the silica-rich, septarian-like concretions found within the syn-rift Saluver Fm. and early post-rift Radiolarian Chert Fm.

3. MATERIAL AND METHODS

The studied concretions were sampled at two sites of the Err nappe: Fuorcla Cotschna and Mal Pass (Fig. 1C). Petrographic studies were carried out by optical microscopy and cathodoluminescence (CL) at the University of Turin (Italy). Oxygen and carbon isotopic compositions of the carbonates were measured at the ETH of Zürich (Switzerland). Fluid

inclusion microthermometry was conducted at the University of Turin (Italy) on primary fluid inclusions (FIs) in quartz and dolomite crystals cementing both veins and septarian cracks.

Sr isotope compositions were measured at the Goethe University of Frankfurt (Germany) on carbonate in thick sections and were compared to those proposed by McArthur et al. (2012) for Jurassic seawater.

Further details about each method are given as supplementary online data.

4. RESULTS: THE SILICA-RICH SEPTARIAN CONCRETIONS

The concretions from the two sites have some features in common and some differences, the latter related to color, lithology and stratigraphic position. In both sites, moreover, they have been found both *in situ* and reworked as clasts within syn-rift turbiditic strata.

4.1 Fuorcla Cotschna

In the Fuorcla Cotschna area, the typical supra-detachment sedimentary basin stratigraphy is preserved (Masini et al., 2011). Here, the Bardella Fm. is lacking and the syn-rift sediments (Saluver Fm.) directly overlie the granitic basement and consist of gravity flow deposits which show a general fining upward trend. The lower part (Figs. 2A-B; Saluver A *sensu* Masini et al., 2011) is mainly composed of clast-supported, locally graded breccias and conglomerates with cm- to dm-sized clasts composed of both Triassic carbonates and granites. Several m-large blocks are also present and consist of Triassic dolostones. Due to the absence of fine grain sediments, bedding is ill defined with bed thickness ranging from dm to m. Upsection, conglomerates and breccia beds, dm to m thick, both clast- and matrix-supported, regularly alternate with thin to medium beds of sandstones and thinly bedded reddish mudrocks (Figs. 2C-

D-E; Saluver B Fm.). Sandstones contain abundant quartz and feldspar grains and subordinated lithic grains of plutonic and metamorphic rocks. Masini et al. (2011) provided a sedimentological interpretation of these sediments and concluded that they are related to different deep water high to low density gravity flows. Microscopic analyses of arenites and rudites show that porosity was strongly reduced by compaction. Carbonate clasts are usually bounded by stylolites, sand grains are tightly packed with long contacts, and the carbonate intergranular cement is scarce. Dissolution seams are observed where a fine-grained clay-rich matrix is present. The Saluver Fm. is overlain by the Radiolarian Chert Fm. (Fig. 2A) It has to be noted that, in spite of the lithostratigraphic unit name, at Fuorcla Cotschna the lower part of the Radiolarian Chert Fm. consists of thinly bedded reddish to grey siliceous mudrocks, grey sandstone, and m-thick polygenic debrite beds interbedded with only subordinated, cm-thick layers of grey cherts (Figs. 2F; 3A-B). The cherts contain ghosts of silicified radiolarian tests. The sandstones, consisting of quartz and feldspar grains, display a looser grain packing than those of the Saluver Fm. and a fine-grained quartz cement (Figs. 3C-D). A finely, μm-sized, crystalline quartz cement is also clearly recognizable in a lenticular, up to 2 m thick, bed of breccia among angular clasts made of Triassic dolostones and subordinated basement rocks (Figs. 2F, 3E-F). In the lowermost part of Radiolarian Chert Fm. (Fig. 2A) a m-large, siliceous concretion has been found; it is enveloped by the host grey sediments documenting a pre-compactional growth (Figs. 4A-C). The concretion is ellipsoidal in shape and over 2 m-long and about 1 m thick It is dark red in color except for the outermost shell which is 10 cm thick and greyish to yellowish in color. The body of the concretion consists of a very fine-grained lithology with a vitreous aspect and conchoidal fracture like cherts. Under the microscope, it is made of very fine-grained quartz crystals (about 10 μm); no radiolarian or sponge spicule ghosts are recognizable (Fig. 4D). Dark patches are

clearly recognizable which consist of concentrations of very fine grained iron oxides and clay minerals. In addition to the large size, a striking feature of the concretion is the occurrence of a dense network of white cracks which gives a brecciated aspect to the rock. Cracks are very irregular, never straight, commonly curved and branching, locally with wedge-shaped terminations. They range in thickness from tens of μm to 2 cm. The geometry of cracks is such that opposing crack surfaces approximately match each other but do not fit exactly, showing that a volume change, namely a shrinkage, during cracking took place. The cracks are filled with isopachous, botryoidal chalcedony, which makes a 1 mm-thick rim along cracks walls, and a mosaic of quartz crystals (up to some mm large, Figs. 4E-F) in the inner parts of the cracks The cracks mainly stop at the outer, yellowish, rim of the concretion. Very similar lithologies (red cherts with white cracks filled with quartz) typify dm-sized clasts occurring within thick, gravelly to sandy, syn-rift turbiditic beds of the Saluver B Fm. i.e. stratigraphically below the base of the Radiolarian Chert Fm. (Figs. 5A-B-C-D). They also consist of red, vitrous, very fine grained siliceous rocks made of microcrystalline quartz with dark patches of iron oxides and clay minerals. Euhedral to subhedral dolomite crystals, 50 to 200 μm in size, are locally scattered in the chert matrix. Roughly circular structures about 100 μm in diameter are locally present which could correspond to radiolarian ghosts. The concretions are internally characterized by two systems of wedge-shaped interconnected crack sets, one concentric, parallel to the edge, and one radial, giving rise to the typical septarian polygonal pattern. The cracks, up to 1 cm wide, are filled with two generations of siliceous cements (Figs. 5E-F). The first is an isopachous rim of chalcedony about 200-300 μm thick, the second is a mosaic of drusy quartz crystals up to 1 mm large elongated perpendicularly to the fracture walls.

The whole syn-rift Saluver Fm. is crossed by subvertical veins filled with quartz and subordinated dolomite (Fig. 6A). Veins are few tens of micron to mm-large showing sharp boundaries where they cross larger clasts in breccia beds. They become more irregular and anastomosed where they pass into the sandstone matrix (Figs. 6B-C). In some instances, these veins are offset by stylolites (Figs. 6D) separating larger clasts.

Quartz veins less than 1 mm thick occur also in the lowermost Radiolarian Chert Fm.; they are recognizable in thin section but hardly in outcrop.

4.2 Mal Pass

In the Mal Pass area, the syn-rift sediments (Saluver Fm.) lie directly over an extensional allochthon with a primary depositional contact (Fig. 7A-B-C). The allochthon is made of Norian peritidal carbonate sediments (Hauptdolomit Fm.) consisting of finely to coarsely crystalline dolostones locally showing fenestral pores filled with a CL zoned dolomite cement. The Saluver Fm., here cropping out for only 10 m of thickness, consists of grey to greenish to reddish finely laminated marly sediments interbedded with cm- to dm-thick beds of breccias. Breccias are both matrix- and clast-supported; clasts are angular and range from some millimeters to up to several centimeters; only locally up to 30 cm large clasts occur. In some layers clasts are very scarce and float in a largely dominant fine-grained matrix. Beds are ill defined and locally show slightly erosional bases. The features of the Saluver Fm. at Mal Pass suggest a relatively deep slope environment affected by hemipelagic sedimentation and debris flow processes (Masini et al.,2011).

The breccias are polimict with clasts mainly composed of Triassic dolostones (Fig. 7D); clasts made of microcrystalline quartz also occur (crystal size around 10 μm). In some of the latter,

dolomite rhombs (50 to 500 μm large) and scattered ghosts of radiolarians are recognizable. In the larger siliceous clasts wedge-shaped, septarian-like cracks filled with coarsely crystalline saddle dolomite and quartz occur (Figs. 8A-B). These clasts closely resemble the reworked fragments of red siliceous septarian concretions described at Fuorcla Cotschna in the middle-upper part of the Saluver Fm.

Fine grained beds consist of marly limestones containing variable amounts of fine sand-sized angular grains of quartz, feldspars, and dolostones and may show parallel lamination. Locally these fine sediments are partially dolomitized with development of rhombs up to 100 μm in size with a dull brown CL luminescence (Figs. 9A-B).

Matrix-supported breccias display dissolution seams particularly evident at the upper and lower boundaries of clasts. The clast-supported breccias are characterized by a tight packing of clasts with long, but not stylolitic, contacts (Figs. 9C, D). The space among clasts is consequently very scarce and almost completely consists of microcrystalline quartz. It could be referred both to a microcrystalline quartz cement of pores or, more likely, to silicification of a fine-grained matrix.

Concretions occur at the base of the syn-rift sequence (Fig. 7C), i.e. just above the top of the extensional allochthon, within grey marly sediments in which locally some millimeter-thick laminae occur. They are coarser and contain fine sand-sized quartz and carbonate lithic grains. The concretions are oblate ellipsoidal in shape (Figs. 7C, 8C), 5 to 20 cm in size and aligned parallel to the bedding. The spacing between individual concretions is commonly less than 20 cm. They consist of a grey hard rock which, depending of the relative amount of dolomite and quartz, could be defined dolomite-bearing chert or siliceous dolostone with orange weathering surfaces. Microscopically, the concretions are made of finely crystalline (μm-sized) dull brown luminescing quartz matrix hosting variable amounts of euhedral to subhedral dolomite crystals, 5

to 30 μm in size and dull to moderate orange luminescing in CL (Figs. 8G-H). Scattered silt- to fine sand-sized detrital quartz grains also occur and no ghosts of biogenic silica remains (radiolarians, sponge spicules) are recognizable. Some of the concretion bodies show a textural heterogeneity where they grew across the mm-thick, bedding parallel fine sand laminae (Figs. 8-F). The concretions are internally cracked with development of a typical pattern of septarian cracks both wedge-shaped, pinching out towards the edge, and concentric, with a maximum width of 5 mm. The cracks-filling phases are quartz and saddle dolomite (Figs. 8D-E-F). Both quartz and dolomite show a very dull brown and moderate orange luminescence respectively and are unzoned. The quartz/dolomite ratio varies from one concretion to the other but is higher than 1; moreover, quartz is always the first crack-filling phase. It forms an isopachous rim of drusy crystals elongated perpendicularly to the fracture walls whereas saddle dolomite, characterized by the typical sweeping extinction, plugs the remaining voids.

A dense network of subvertical, up to 5 cm-wide and m-long veins filled with mm-large saddle dolomite and quartz crystals crosscutting the Triassic dolostones, occurs in the allochthon and is truncated at its top. The same kind of veins are also preserved within the dolomitic clasts of the Saluver Fm. breccias documenting their formation before the deposition of mass flow deposits in which they are enclosed. Quartz crystals are dull brown in CL whereas dolomite shows a bright to dull orange, mostly homogeneous, luminescence. Despite visible only under the microscope, quartz veins also occur in the Saluver Fm. In fact they are irregular veinlets 10's of microns-thick that cross subvertically the breccia beds; they do not cut through clasts but follow their edges (Figs. 9C-D).

4.3 Fluid inclusion and stable isotopes

In order to constrain nature, composition, origin, temperature, and circulation pathways of fluids responsible for precipitation of quartz and dolomite in siliceous concretions, cracks, and veins, different analytical method were applied. No primary fluid inclusions of suitable size were found in the siliceous cements of septarian concretions at Fuorcla Cotschna (Figs. 10A-C). Moreover, because of the absence of a sufficient amount of carbonate material, also O, C and Sr isotope analyses could not be performed. Consequently, fluid inclusion microthermometry and isotope analyses were accomplished only on samples from the Mal Pass section.

Primary fluid inclusions were found in saddle dolomite and quartz cements of septarian cracks and veins. Homogenization temperatures (T_h) of septarian crack filling phases show the following values: 140°C-150°C (highest frequency) for quartz and 150-160°C for dolomite (Fig. 3B; 4). Homogenization temperatures of FIs in veins range from 130-140° C for quartz cement and from 140-150°C for saddle dolomite (Figs. 11). The carbonate fraction (dolomite) of the septarian concretions, both as concretion body and crack-filling cement, has been analyzed for stable oxygen, carbon and strontium isotopes. All the analyzed samples show slightly positive $\delta^{13}C$ values of 0.2‰ to 1.00‰ (VPDB) and negative $\delta^{18}O$ values of -6.8‰ to -10.2‰ (VPDB; Fig. 12). In particular, the most depleted $\delta^{18}O$ values are found in the crack-filling dolomite. $^{87}Sr/^{86}Sr$ ratios for dolomite cements show values ranging between 0.707734±0.000129 and 0,709291±0,000119 which are thus strongly higher than the highest value reported for Middle-Late Jurassic seawater (0.70730± McArthur et al., 2012).

5. DISCUSSION

The studied concretions show a wide range of features, including stratigraphical relationships, petrographic characteristics and geochemical signatures, which enable to draw an unconventional scenario in the field of concretionary growth in sedimentary successions. The set of features will be discussed below in order to constrain the mechanisms of formation and the geological context in which the concretions developed.

5.1 Shallow burial formation

A first strong constraint comes from the septarian cracked concretions found as clastsin the Saluver Fm. at both Fuorcla Cotschna and Mal Pass. The angular edges and the contrast between the gravelly sand texture of the bed in which they are enclosed and the very fine grain size of the siliceous concretions demonstrate that they were not formed in the bed where they occur but firstly formed in fine grained sediments before being reworked. The possibility that these siliceous concretions were reworked from older formations exposed along fault planes during the tectonic evolution of the Adriatic continental margin can be excluded. The only cherts older than the Saluver Fm. occur in the Agnelli Fm. They are grey in color and consist of echinoderm-bearing, sponge-spicule-rich sediments. Spicules are clearly recognizable both in cherts where they are preserved as microquartz or chalcedony, and in limestones where are replaced by sparry calcite which filled moldic voids due to opal A dissolution (Figs. 13A-B-C). None of these features are recognizable in the siliceous clasts reworked in the Saluver Fm. at both Fuorcla Cotschna and Mal Pass. Therefore, they only could form in the Saluver Fm. as concretions generated by precipitation of microcrystalline quartz in the pores of very fine grained, clay-rich sediments. This constrains their formation to a shallow burial, at a depth in the reach of gravity-related, submarine erosion processes, likely from some meters to few tens of meters of burial at

most. Evidence for reworking of concretions from mudstone or sandstone successions has been reported in literature (e.g. Hesselbo and Palmer, 1992; Garcìa-Garca et al., 2013) and a shallow burial concretionary growth was inferred. The occurrence of borings at the edge of the reworked concretions led the authors to infer full lithification before reworking. An early formation of cracks is further supported by the observation of septarian concretions enclosed in recent sediments with maximum burial of 10-12 m (Duck, 1995).

The *in situ* Mal Pass concretions occurring at the base of the Saluver Fm., as well as the m-large Fuorcla Cotschna one, at the base of the Radiolarian Chert Fm., conversely show ellipsoidal shapes, smooth outer edges and the same fine-grained texture as the surrounding sediments: this demonstrates that they were not reworked and still occur in their primary position. A second significant feature of the studied concretions is provided by the septarian crack fills. No sediments but only authigenic minerals are found in the cracks (Figs. 4E-F, 5A-B-E-F, 8C-D-E-F). This would not be expected for a concretion with quite large open cracks being reworked, fragmented, and involved in a high-density mass flow. Therefore, not only did the concretions start to grow at very shallow burial depth but also the cracks had to be formed and completely filled before reworking.

5.2 Source of silica

The silica-rich composition of the concretions (mixed dolomite and chert at Mal Pass or nearly pure chert at Fuorcla Cotschna) raises a question about the origin of silica, considered that they developed in terrigenous sediments (Saluver Fm.). A siliceous allochemical fraction indeed does occur in the fine-grained beds as ghosts of microquartz-filled radiolarians. However, they are very scarce and scattered, and even in the Radiolarian Chert Fm. radiolarian-bearing cherts occur

only as cm-thick beds largely subordinated to sandstones and mudstones (Figs. 3A-B). The amount of biogenic silica was thus simply not enough to fill the high porosity of nearly uncompacted fine sediments and the networks of cracks in concretions. Moreover, the opal A-opal CT-quartz transformations, have been shown to take place at temperatures and burial depths (at least some hundred meters e.g. Keller & Isaacs, 1985) which are incompatible with the shallow burial (some meters to very few tens of meters) reasonably required for erosional reworking. This is especially true in siliceous sediments rich in a detrital clay fraction which has the effect of lowering the rate of diagenetic reactions and thus delays to deeper burial silica polymorphs transformations (Kastner et al., 1977; Isaacs, 1982). All these observations strongly suggest that silica could not be sourced by redistribution of the biogenic opal of radiolarian skeletons contained within the concretion-hosting beds. The same conclusion was reached on the basis of mass balance calculations even for pelagic cherty limestones by Lawrence (1994). In that case the origin of a great part of silica was individuated in the diagenetic alteration of clay minerals contained in the underlying stratigraphic succession consisting of thick mudstones. Such source is not available in the study area where the Saluver Fm., mainly made of breccias, conglomerates and sandstones, contains only minor amounts of clay. Another possibility for cross-stratigraphic flow of silica-rich fluids considers the release of water as opal-A is converted to opal-CT. This causes overpressure development resulting in hydrofracturing, clastic injections, and pockmarks at the sea floor (e.g. Monterey Fm.: Eichhubl & Behl, 1998; Eichhubl & Boles, 2000; Shetland Basin: Davies et al., 2008). However, this model requires biosiliceous formations several hundred meters thick and again does not apply to the Saluver Fm. which is much thinner and nearly barren of biogenic silica. A more likely hypothesis for the study case concerns the intervention of fluids involved in much larger circulation pathways (i.e. interacting

with the underlying cataclastic granitic basement) Important indications in this sense are provided by $^{87}Sr/^{86}Sr$ ratios of the saddle dolomite filling septarian cracks at Mal Pass, which are higher than those of Middle-Late Jurassic seawater (McArthur et al., 2012) documenting strong fluid interactions with minerals containing abundant radiogenic ^{87}Sr such as feldspars. This hypothesis is also supported by microthermometry of primary fluid inclusions and stable isotope data from the Mal Pass area (Figs. 11, 12).

No fluid inclusion data are obviously available for the fine-grained quartz of the chert matrix, but they could be obtained from quartz and dolomite cements in the septarian cracks and veins. They provide homogenization temperatures with a histogram mode around ~150°C (Fig. 11). Actually, a dispersion of values is observed on a wider range. This is most likely due to the impossibility to distinguish assemblages of primary fluid inclusions referable to different, subsequent, entrapment events (FIAs) characterized by temperature oscillations.

O and C isotopes (**Fig. 12**) in the saddle dolomite further confirm circulation of fluids in the granitic basement. Carbon isotope compositions close to 0‰ VPDB are typical for normal seawater with no contribution from organic matter degradation. The O isotopes values ($\delta^{18}O$ from -6 ‰ to -10‰ VPDB) combined with the T_h of dolomite allow to calculate the $\delta^{18}O$ of the parent fluids by using the Horita (2014) equation. This back calculation yields values ranging from +3 to +7‰ SMOW. This enrichment compared to normal seawater can be explained by several mechanisms: evaporation of sea water (e.g. McKenzie, 1979), clay mineral diagenesis (e.g. Dählmann and de Lange, 2003; Hensen et al., 2007), gas hydrate dissociation (e.g. Aloisi et al. 2000), fluid-rock interaction with silicate minerals of siliciclastic or crystalline rocks (e.g. Haeri-Ardakani et al., 2013). Given the geological context of a deep marine basin, evaporation is ruled out; the overall reduced thickness of syn-rift sediments overlying the detachments fault and

the absence of mud-rich as well as organic-rich sediments in the Saluver Fm. also exclude clay mineral transformations and gas hydrate formation respectively. The ^{18}O enrichment in dolomite, combined with the high $^{87}Sr/^{86}Sr$ ratios, is better explained by water-rock interaction with felsic crustal rocks: oxygen isotope exchanges take place during alteration of feldspars and lead to enrichment of heavy isotopes in the fluid (e.g. Pirajno 2009).

These data, considered together with common reworking of concretions, in turn documenting formation of the septarian cracked concretions at shallow burial depths, may only be explained taking into account hydrothermal fluids: the latter were heated and enriched in silica during circulation within the crystalline basement and then flowed upwards crossing the already deposited Saluver Fm. beds to ultimately percolate through sub-bottom sediments (Fig. 14). This is also documented by the style of veins which in fact crosscut with sharp boundaries the coherent portions of the succession (e.g. the Triassic dolostone allochthon at Mal Pass and the clasts in the breccias and conglomerates of the Saluver Fm. at Fuorcla Cotschna) but become more irregular where crossing the sandstone matrix of breccias/conglomerates. Veins subdivide into a number of smaller veinlets turning around clasts or even apparently stopping at the clast/matrix boundary (Figs. 9C, D). Moreover, veins are commonly offset by stylolitic boundaries among carbonate clasts documenting that veins formed in sediments which had already acquired a degree of coherence due to mechanical compaction but before the sediment overburden was thick enough to trigger pressure dissolution processes (Figs. 6 D). The style of quartz and quartz-dolomite veins therefore shows that they did not develop in fully lithified rocks during Alpine deformation but in only partially coherent sediments in Jurassic times during Saluver or Radiolarian Chert formations deposition.

5.3 Evolutionary model and flow pathways

Integrating the tectono-stratigraphic evolution of the studied succession (Masini et al., 2011) with the body of evidence discussed above, the following scenario may be envisaged for the formation of the silica-rich septarian concretions . During the middle Early Jurassic rifting stage, fault activity localized in the future distal domain. The style of deformation changed from pure shear, high-angle faulting (stretching) to crustal and lithospheric thinning to hyper-extension associated with detachment faulting and exhumation of basement and mantle rocks at the seafloor. The simultaneous lithospheric thinning resulted in high thermal gradients (Mohn et al. 2010) that, together with the high permeability due to active faulting, favored hydrothermal circulation in a basin that was at deep marine conditions (Masini et al., 2011; Pinto et al. 2015). Very high heat fluxes have been indeed detected in present day distal continental margins (e.g. South China Sea Sun et al., 2018a, b).

Seawater deeply penetrated the substrate through fractured zones of fault systems (Fig. 14), which gave rise to fluid convection cells (e.g. Hollis et al. 2017). The result of this circulation in the hyperextended Adriatic margin was an increase of fluid temperature and an enrichment in ions liberated by the breakdown of silicate minerals within the faulted basement along the detachment fault. In their way up through the sedimentary column, these over-pressured silica-rich fluids opened their way in compact, partially lithified sediments giving rise to quartz veins (e.g. Bons, 2001). Approaching the seafloor, the flow crossed soft and uncompacted sediments. Fluid flow cooled down and became likely more diffuse causing: i) a very limited degree of dolomitization of the existing albeit minor carbonate sediment fraction followed by; ii) micro-quartz precipitation in the primary pores of discrete volumes of fine clay-rich sediments. Where

the original host sediment was a marl (i.e. the Mal Pass *in situ* concretions), in addition to microquartz precipitation in the pores, a replacement of the undolomitized fraction of carbonate sediment by silica may be supposed. Because of the greater resistance of dolomite to dissolution (e.g. Lawrence, 1994), the previously formed dolomite crystals were not silicified and are now clearly recognizable in the surrounding microquartz matrix. This resulted in the formation of siliceous concretions strongly similar to diagenetic products developed in biogenic silica-rich sediments. iii) Cementation of cracks in septarian concretions with chalcedony and quartz and, locally (Mal Pass), saddle dolomite.

Recurrent gravity flow processes, taking place along the slopes of the topographically rugged supra-detachment basin, affected the Saluver Fm. involving also the just formed siliceous concretions, which were broken into clasts and incorporated into the gravity flow (Figs. 5D, 8A).

Given that data support an early genesis of concretions very close to the sediment-water interface as a result of silica-rich hydrothermal fluid flow in unconsolidated sediments, it could be suggested that their formation was possibily related to submarine hydrothermal vents comparable to hot springs such as the ones reported at the bottom of the Yellowstone Lake (Shanks et al, 2005). The latter include morphologies such as tabular bodies, and tubular and branching structures representing fluid conduits. Mixing of hot silica-rich fluids with the cold lake floor waters causes precipitation of amorphous silica within soft sediments beneath and at the sediment-water interface. The overall texture of these features resembles the precipitation of silica on bacterial filaments as documented in other hydrothermal systems (e.g. Jones et al., 1997). The concretions under study do not show either the morphologies nor the internal microtextures of the above mentioned subaqueous vents. They could thus represent the products of silica precipitation from fluids flowing up within sub-sea floor sediments closely below

hydrothermal vents. in the same way as methane-rich fluids give rise to carbonates characterized by chemosynthetic fossil associations at seep sites on the sea bottom but only to masses of cemented sediments in the underlying sediment column (e.g. Clari et al., 2009). As to the mechanisms of septarian cracking, this was not the focus of the present contribution. However, some constraints come out of the data acquired.

1) Growth of concretions and cracking took place at shallow depths of burial, as common reworking of concretions shows; this implies that fluid overpressuring related to significant burial cannot be considered a generalized genetic mechanism for septarian cracking (e.g. Astin and Scotchman, 1988; Sellés Martìnez, 1996; Hounslow, 1997; Behl, 2011).

2) concretions with septarian-like cracks developed in fine grained sediments, either of nearly pure clayey or marly composition; none of them occur in the much more permeable sand-sized or coarser sediments. The occurrence of thin sand-bearing laminae in fine sediments conversely did not disturb the development of concretions. This strongly suggests that the fine grain size of host sediments seems to play a fundamental role in growth of this kind of concretions.

As suggested by several authors (Hendry et al., 2006) syneresis of clay-rich sediments is one of the mechanisms proposed for septarian cracking but changes in pore water salinity are considered fundamental in triggering syneresis (e.g. McMahon et al., 2016). This led some authors (e.g. Pratt, 2001) to reject syneresis as a cause for septarian cracking. Fluids flowing upwards after a deep circulation path and intense chemical exchanges with basement rocks, however, have acquired a salinity significantly higher than the seawater contained in the pores of shallow buried, fine-grained sediments. This is likely enough to cause shrinkage and consequent cracking. The ^{87}Sr-and ^{18}O-enriched fluids responsible for growth of the studied concretions could have corresponded to such a brine and had the potential to trigger septarian cracking.

Lastly, other two mechanisms have been suggested. One takes into account seismic shocks as triggering mechanism of cracking (Pratt, 2001). The other is related to water loss upon transformation of amorphous silica gels into quartz or chalcedony in hydrothermal ores (e.g. Saunders, 1990, Herrington & Wilkinson, 1993; Prokofiev et al., 2017). Given the tectonically active context of the study area, being located in the former Adriatic distal rifted margin, the siliceous composition of concretions, and the existence of a hydrothermal circulation, both hypotheses could be possible but on the basis of the available data none of them can be either confirmed or rejected.

6. **CONCLUSIONS**

Unconventional quartz-rich concretions, strongly resembling radiolarian cherts, with or without septarian cracks, may be found in sedimentary successions in which biogenic silica is scarce or even substantially absent. We propose that silica-rich fluids originated from convection cells of seawater deeply penetrating within fault-related fracture zones developed in the substrate of the basin characterized by anomalous thermal gradients due to hyperthinning of continental crust.. Fluids were heated, enriched in silica, and circulated upwards. . Fractures were generated by this flow of overpressured fluids while crossing coherent sediments Higher up in the sediment column, just below the sea floor, a microquartz cement precipitated in soft, highly porous sediments, giving rise to silica-rich concretions. Fractures therefore acted as the feeding system connnecting the source of silica and hot fluids, i.e.the basement, with venting sites that likely existed at the sea floor. No record of these vents is preserved but the siliceous concretions likely represent the loci of precipitation within sediments immediately below vents. Syneresis processes, related to the presence of clay minerals in host sediments and possibly triggered by

the advection of basement-derived brines, generated septarian cracks which were quickly filled with quartz and locally saddle dolomite cements. The occurrence of concretions reworked in gravity flow deposits confirms that septaria can commonly form at shallow burial depths.

In orogenic contexts, like those usually studied in outcrops, chert concretions and quartz veins are treated separately, the former being commonly interpreted as due to “normal” diagenetic processes in deep marine environments whilst the latter is related to compressional tectonics. We propose that veins and concretions may be the result of diagenetic processes coeval with, and genetically related to, a syn-depositional tectonically-driven circulation of hydrothermal fluids, which took place prior to convergence and orogenic processes. Siliceous concretions may thus be a diagnostic tool to unravel fluid flow and thermal evolution along distal deep water hyper-extended rifted margins.

ACKNOWLEDGMENTS

The research was financed through a grant to Gianreto Manatschal by Petrobras S.A., MM4 Consortium (BP, Conoco Phillips, Statoil, Petrobras, Total, Shell, BHP-Billiton, and BG) and Università Italo-Francese/Université Franco-Italienne (Bando Vinci 2014, C2-190 to Nicolò Incerpi). Many thanks to the reviewers James P. Hendry (UK) and Josè Sellès Martìnez (Argentina) for the thorough and detailed revision and precious suggestions which greatly improved the text.

REFERENCES

Aloisi, G., Pierre, C., Rouchy, J.M., 2000. Methane-related authigenic carbonates of eastern Mediterranean Sea mud volcanoes and their possible relation to gas hydrate destabilitzation: Earth and Planetary Science Letters, 184, 321-338.

Astin, T.R., Scotchman, I.C., 1988. The diagenetic history of some septarian concretions from the Kimmeridge Clay, England: Sedimentology, v. 35, p. 349-368.

Barrett, T.J., 1981. Chemistry and mineralogy of Jurassic bedded chert overlying ophiolites in the North Apennines, Italy: Chemical Geology, v. 34, p. 289-317.

Behl, R., 2011. Chert spheroids of the Monterey Formation, California (USA): Early-diagenetic structures of bedded siliceous deposits: Sedimentology, v. 58(2), p. 325-351.

Clari, P., Dela Pierre, F., Martire, L., Cavagna, S., 2009. The Cenozoic CH_4-derived carbonates of Monferrato (NW Italy): A solid evidence of fluid circulation in the sedimentary column: Marine Geology, v. 265, p. 167-184.

Bons, P.D., 2001. The formation of large quartz veins by rapid ascent of fluids in mobile hydrofractures: Tectonophysics, v. 336, p. 1-17.

Breitenbach, S.F.M., Bernasconi, S.M., 2011. Carbon and oxygen isotope analysis of small carbonate samples (20 to 100 µg) with a GasBench II preparation device: Rapid Communications in Mass Spectrometry, v. 25, p. 1910-1914.

Dählmann, A., de Lange, G.J., 2003. Fluid-sediment interactions at Eastern Meditterranean mud volcanoes: a stable isotope study from ODP Leg 160: Earth and Planetary Science Letters, v. 212, 377-391.

Davies, R.J., Goulty, N.R., Meadows, D., 2008. Fluid flow due to the advance of basin-scale silica reaction zones: Geological Society of America Bulletin, v. 120, p. 195-206.

Duck, R.W., 1995. Subacqueous shrinkage cracks and early sediment fabrics preserved in Pleistocene calcareous concretions: Journal of the Geological Society, v. 52, p. 151-156.

Eichhubl, P., Behl, R.J., 1998. Diagenesis, deformation, and fluid flow in the Miocene Monterey Formation, in Eichhubl, P., ed., Diagenesis, deformation, and fluid flow in the Miocene Monterey Formation of Coastal California: Los Angeles, Pacific Section, Society for Sedimentary Geology (SEPM) Special Publication 83, p. 5–13.

Eichhubl, P., Boles, J.R., 2000. Focused fluid flow along faults in the Monterey Formation, coastal California: Geological Society of America Bulletin, v. 112, p. 1667–1679, doi: 10.1130/0016-7606(2000)112<1667:FFFAFI>2.0.CO;2.

Garcìa-Garcìa, F., Marfil, R., De Gea, G.A., Delgado, A., Kobstädt, A., Santos, A., Mayoral, E, 2013. Reworked marine sandstone concretions: a record of high-frequency shallow burial to exhumation cycles: Facies, v. 59, 843-861.

Goldstein, R.H., Reynolds, T.J., 1994. Systematics of fluid inclusions in diagenetic minerals: SEPM Shourt Course 31, Tulsa, p. 199.

Gross, G.A., 1972. Primary features in cherty iron-formation: Sedimentary Petrology, v. 7, p. 241-261.

Haeri-Ardakani, O., Al-Aasm, I., Coniglio, M., 2013. Fracture mineralization and fluid flow evolution: an example from Ordovician-Devonian carbonates, southwestern Ontario, Canada: Geofluids, v. 13, 1-20.

Hendry, J.P., Pearson, M.J., Trewin, N.H., Fallick, A.E., 2006. Jurassic septarian concretions from NW Scotland record interdependent bacterial, physical and chemical processes of marine mudrock diagenesis: Sedimentology, v. 53, p. 537-565.

Hensen, C., Nuzzo, M., Hornibrook, E., Pinheiro, L., Bock, B., Magalhaes, V., Bruckmann, W., 2007, Sources of mud volcano fluids in the Gulf of Cadiz-indications fro hydrothermal imprint: Geochimica et Cosmochimica Acta, v. 71, 1232-1248.

Herrington, R.J., Wilkinson, J.J., 1993. Colloidal gold and silica in mesothermal vein systems: Geology, v. 21, p. 539-542.

Hesselbo, S.P., Palmer, T.J., 1992. Reworked early diagenetic concretions and the bioerosional origin of a regional discontinuity within the British Jurassic marine mudstones: Sedimentology, v. 39, p. 1045-1065.

Hollis, C., Bastesen, E., Boyce, A., Corlett, H., Gawthorpe, R., Hirani, J., Rotevatn, A., Whitaker, F., 2017. Fault-controlled dolomitization in a rift basin: Geology, v. 45/3, p. 219-222.

Horita, J., 2014. Oxygen and carbon isotope fractionation in the system dolomite-water-CO_2 to elevated temperatures: Geochimica et Cosmochimica Acta, v. 129, p. 111-124.

Hounslow, M.W., 1997. Significance of localized pore pressures to the genesis of septarian concretions: Sedimentology, v. 44, p. 1133-1147.

Incerpi, N., 2017. Hydrothermal systems in distal rifted margins and their role in the thermal evolution of sedimentary successions. Study of two fossil analogues in the Swiss Alps and Pyrenees: PhD Thesis, p. 245, University of Turin (Italy) and University of Strasbourg (France) available online at https://tel.archives-ouvertes.fr/tel-01838600

Incerpi, N., Martire, L., Manatschal, G., Bernasconi, S.M., 2017. Evidence of hydrothermal fluid flow in a hyperextended rifted margin: the case study of the Err nappe (SE Switzerland): Swiss Journal of Geosciences, doi: 10.1007/s00015-016-0235-2.

Isaacs, C.M., 1982. Influence of rock composition on kinetics of silica phase changes in the Monterey Formation, Santa Barbara area, California: Geology, v. 10, p. 304–308, doi: 10.1130/0091-7613(1982)10<304:IORCOK>2.0.CO;2.

Jones, B., Renault, R.W., Rosen, M.R., 1997. Biogenicity of silica precipitation around geysers and hot-spring vents, North Island, New Zealand: Journal of Sedimentary Research, v. 67, p. 88-104.

Kastner, M., Keene, J.B., Gieskes, J.M., 1977. Diagenesis of siliceous oozes–I. Chemical controls on the rate of opal-A to opal-CT transformation-An experimental study: Geochimica et Cosmochimica Acta, v. 41, p. 1041-1059, doi: 10.1016/0016-7037(77)90099-0.

Keller, M.A., Isaacs, C.M., 1985. An evaluation of temperature scales for silica diagenesis in diatomaceous sequences including a new approach based on the Miocene Monterey Formation, California: Geo-Marine Letters, v. 5, p. 31–35, doi: 10.1007/BF02629794.

Lawrence, M.J.F., 1994. Conceptual model for early diagenetic chert and dolomite, Amuri Limestone Group, north-eastern South Island, New Zealand: Sedimentology, v. 41, 479-498.

Manatschal, G., 1999. Fluid- and reaction-assisted low-angle normal faulting: evidence from rift-related brittle fault rocks in the Alps (Err Nappe, eastern Switzerland): Journal of Structural Geology, v. 21, 777-793.

Manatschal, G., MArquer, D., Frueh-Green, G.L., 2000. Channellised fluid flow and mass transfer along a rift-related detachment fault (Eastern Alps, southeast Switzerland): Geological Society of America Bulletin, v. 112, 21-33.

Masini, E., Manatschal, G., Mohn, G., Ghienne, J.F., Lafont, F., 2011. The tectono-sedimentary evolution of a supra-detachment rift basin at a deep-water magma-poor rifted margin: the

example of the Samedan Basin preserved in the Err nappe in SE Switzerland: Basin Research, v. 23, p. 652-677.

McArthur, J.M., Howarth, R.J., Shields, G.A., 2012. Strontium Isotope Stratigraphy. In: Gradstein F.M., Ogg J.G., Schmitz M., Ogg G. (Eds.), The Geologic Time Scale 2012, p. 127-144, Elsevier.

McKenzie, J.A., 1979. Holocene dolomitization of calcium carbonate sediments from the coastal sabkhas of Abu Dhabi, UAE: a stable isotope study: Journal of Geology, v. 89, 185-198.

McMahon, S., van Smeerdijk Hood, A., McIlroy, D., 2016. The origin and occurrence of subaqueous sedimentary cracks. In: Brasier, A. T., McIlroy, D. &McLoughlin, N. (eds) Earth System Evolution and Early Life: a Celebration of the Work of Martin Brasier. Geological Society, London, Special Publications, 448, https://doi.org/10.1144/SP448.15.

Mohn, G., Manatschal, G., Müntener, O., Beltrando, M., Masini, E., 2010. Unraveling the interaction between tectonic and sedimentary processes during lithospheric thinning in the Alpine Tethys margins: International Journal of Earth Sciences, v. 99, p. 75-101.

Mohn, G., Manatschal, G., Masini, E., 2011. Rift-related inheritance in orogens: a case study from the Austroalpine nappes in Central Alps (SE-Switzerland and N-Italy): International Journal of Earth Sciences, v. 100(5), p. 937-961.

Mohn 2012. Necking of continental crust in magma-poor rifted margins: Evidence from the fossil Alpine Tethys margins: Tectonics, v. 31, TC1012, doi:10.1029/2011TC002961.

Mozley 2003. Diagenetic structures. In: Middleton V. G. (Ed.) Encyclopedia of sediments and sedimentary rocks, 219-225, Springer.

Pinto, V.H., Manatschal, G., Karpoff, A.M., Viana, A., 2015. Tracing mantle-reacted fluids in magma-poor rifted margin: The example of Alpine Tethyan rifted margin: Geochemistry, Geophysics, Geosystems, v. 16, p. 3271-3308.

Pirajno, F., 2009. Hydrothermal processes and mineral systems: Springer, https://doi.org/10.1007/978-1-4020-8613-7 , 1250 p.

Pratt, B.R., 2001. Septarian concretions: internal cracking caused by synsedimentary earthquakes: Sedimentology, v. 48, p. 189-213.

Prokofiev, V.Y., Kamenetsky, V.S., Selektor, S.L., Rodemann, T., Kovalenker, V.A., Vatsadze, S.Z., 2017. First direct evidence for natural occurrence of colloidal silica in chalcedony-hosted vacuoles and implications for ore-forming processes: Geology, v. 45, p. 71-74.

Saunders, J.A., 1990. Colloidal transport of gold and silica in epithermal precious-metal systems: evidence from the Sleeper deposit, Nevada: Geology, v. 80, p. 757-760.

Selles-Martinez, J., 1996. Concretion morphology, classification and genesis: Earth Science Reviews, v. 41, p. 177-210.

Selles-Martinez, J., 1998. The overpressured-undercompacted cell path, an alternative model for concretionary growth: Bulletin Elf-Aquitaine, Memoire (Overpressures in Petroleum Exploration), p. 93-97.

Schubel, K.A., Simonson, B.M., 1990. Petrography and diagenesis of cherts of Lake Magadi, Kenya: Journal of Sedimentary Petrography, v. 60, p. 761-776.

Shanks, W.C.P. III, Morgan, L.A., Balistrieri, L., Alt, J.C., 2005. Hydrothermal vent fluids, siliceous hydrothermal deposits, and hydrothermally altered sediments in Yellowstone Lake. In: Inskeep WP and McDermott TR (eds) Geothermal biology and geochemistry in Yellowstone National Park: proceedings of the Thermal Biology Institute workshop,

Yellowstone National Park, WY, October 2003. Montana State University publications, p. 53-72.

Sun, Z., Jian, Z., Stock, J.M., Larsen, H.C., Klaus, A., Alvarez Zarikian, C.A., and the Expedition 367/368 Scientists, 2018a. Proceedings of the International Ocean Discovery Program Volume 367/368 publications.iodp.org https://doi.org/10.14379/iodp.proc.367368.103.2018

Sun, Z., Jian, Z., Stock, J.M., Larsen, H.C., Klaus, A., Alvarez Zarikian, C.A., and the Expedition 367/368 Scientists, 2018b. Proceedings of the International Ocean Discovery Program Volume 367/368 publications.iodp.org https://doi.org/10.14379/iodp.proc.367368.105.2018

Weissert, H.J., Bernoulli, D., 1985. A transform margin in the Mesozoic Tethys: evidence from the swiss alps: Geologische Rundschau, v. 74, p. 665-679.

Wilson, R.C.L., Manatschal, G., Wise, S., 2001. Rifting along non-volcanic passive margins: stratigraphic and seismic evidence from the Mesozoic successions of the Alps and western Iberia: Geological Society of London, Special Publications, v. 187(1), p. 429-452.

FIGURE AND TABLE CAPTIONS

Figure 1. (A) Simplified tectonic map of SE Switzerland showing the distribution of the main Alpine nappes (Austroalpine and Penninic; modified after Mohn et al., 2012) as well as (B) the distribution of former rift domains in the present-day Alpine nappe stack. (C) Schematic restored section across the Adriatic continental margin at Middle Jurassic time (section a-a’ in B). The

different paleogeographic rift domains of the Adriatic rifted margin and the former locations of the two study areas (Fuorcla Cotschna and Mal Pass) are also shown.

Figure 2. (A) Schematic, not to scale, stratigraphic log of Fuorcla Cotschna area. (B) Saluver A Fm. Poorly organized, clast-supported sedimentary breccia with cm- to dm-sized clasts made of Triassic carbonates and granites. The scarce matrix is made of quartz-feldspar sand. (C) The Saluver B Fm. is composed of graded, dm- to m-thick beds of matrix-supported breccia with clasts made of both carbonates and basement-derived material. (D-E) The uppermost Saluver B Fm. is characterized by alternation of subordinated thinly bedded reddish mudrocks with thin to medium beds (D) and medium to thick beds (E) of sandy to gravelly turbidites. (F) Meter-thick, lenticular, breccia bed occurring within the lowermost part of the Radiolarian Chert Fm. It is clast-supported with angular clasts of Triassic dolostones and subordinated basement rocks ranging in size from cm- to dm. Note that the blackish portions represent the siliceous cement of the breccia.

Figure 3. Fuorcla Cotschna area: (A-B) Outcrop photograph and line drawing of the basal part of Radiolarian Chert Fm. here mainly consisting of alternances of mudrocks and sandstones with only lesser cherty beds. Encircled scale in the centre is 5 cm long. (C) Transmitted light and (D) crossed polars photomicrographs showing sandstone beds in the lowermost part of the Radiolarian Chert Fm. made of quartz and feldspar grains. The intergranular pores are occupied by fine-grained quartz in which Fe-oxide-filled rhombs occur. They are possibly related to weathering of Fe-rich dolomite. The whole rock is crosscut by thin quartz veins. (E) Transmitted

light and (F) crossed polars photomicrographs showing the microquartz cement of the m-thick lenticular breccia bed occurring in the lowermost part of the Radiolarian Chert Fm.

Figure 4. Fuorcla Cotschna area. (A-B) Meter-scale red siliceous concretion within the lowermost part of the Radiolarian Chert Fm. here consisting of grey, thinly bedded mudrocks. The hammer is about 30 cm long. (C) Detail of the cm-large, randomly oriented, quartz-filled septarian-like cracks affecting the concretion body. (D) Transmitted light (inset) and crossed polars photomicrographs of the fully silicified, radiolarian-free, body of the concretion. (E) Transmitted light and (F) crossed polars photomicrographs of the chalcedony- and drusy quartz-filled concretion cracks.

Figure 5. (A-B-C) Hand specimens of dm-large red siliceous concretions characterized by mm- to cm-large, wedge shaped and concentric, septarian cracks cemented by quartz. These concretions are hosted as clasts within the gravelly tubiditic Saluver B Fm. (D). (E) Transmitted light and (F) crossed polars photomicrographs of a reworked clast of septarian concretion in the Saluver B Fm. The body of the concretions consist of extremely finely crystalline quartz with black inclusions made of clay and iron oxides. Septarian cracks are filled by a first rim of isopachous, botryoidal chalcedony and a second drusy quartz cement.

Figure 6. (A) The Saluver A Fm. conglomerates and breccias are crosscut by randomly oriented, m-long and up to mm-wide, quartz-dolomite veins. Note that both the quartz-rich sandy matrix of breccias and veins weather out with respect to the carbonate clasts. Transmitted light (B) and crossed polars (C) photomicrographs showing quartz-dolomite veins crosscutting carbonate

clasts and sandstone matrix in conglomerate beds. The vein boundaries are sharp within the clasts whilst less well-defined within the matrix. (D) Transmitted light photomicrograph showing quartz veins crosscutting a conglomerate with carbonate clasts and sandstone matrix. Note that the veins are locally offset by stylolites.

Figure 7. (A) Schematic, not to scale, stratigraphic log of Mal Pass area. (B) Primary stratigraphic contact between the extensional allochthon made of Triassic dolomites and the Jurassic syn-rift Saluver Fm. The overturned setting is due to Alpine tectonics. (C) The first decimeters of the Saluver Fm. are characterized by the occurrence of cm- to dm-large septarian concretions within a grey marly sediment. (D) Decimeter-thick beds of sedimentary breccias made of cm- to dm-large Triassic carbonate clasts as well as basement rocks. A m-scale block of Triassic dolostones is visible in the center.

Figure 8. Mal Pass area. (A) Outcrop photograph and (B) detail of a dm-large clast within the Saluver Fm. It consists of a siliceous concretion showing septarian-like cracks filled with saddle dolomite and quartz. (C) Polished slab of a cm-large septarian concretion. It is characterized by wedge-shaped radial and concentric cracks filled with quartz and saddle dolomite cements. (D) Transmitted light and (E-F) crossed polars microphotographs of a septarian concretion whose cracks are cemented by a first rim of quartz (QTZ) followed by saddle dolomite (DOL). Transmitted light (G) and crossed polars (H) photomicrographs of the siliceous body of the concretions which show scattered, tens of μm large, rhombs of dolomite surrounded by very finely crystalline quartz.

Figure 9. Mal Pass area. (A) Transmitted light photomicrograph of partially dolomitized, finely arenitic beds in the Saluver Fm. (B) Closeup in cathodoluminescence of (A) showing dull brown dolomite rhombs. (C) Transmitted light and (D) crossed polars photomicrographs of lithoclastic breccias of the Saluver Fm. A microquartz matrix and quartz veinlets several tens of μm-large running along the clast edges are recognizable.

Figure 10. (A) Primary fluid inclusions within a quartz crystal cementing the dolomite-quartz veins crosscutting the extensional allochthon at Mal Pass. (B) Quartz cement of a septarian crack in a concretion at Mal Pass. Both primary and secondary fluid inclusions are here preserved and easily discernible. (C) Quartz cement of a septarian crack in a siliceous concretions at Fuorcla Cotschna. Arrows show the several trails of secondary fluid inclusions crosscutting each other as well as the crystals boundaries. Note that: independently of the studied area and samples, inclusions are always very small in size (below 2 μm); only heating cycles could be performed which provided homogenization temperatures; no growth zones are recognizable in crystals.

Figure 11. Histogram of the homogenization temperatures for quartz and dolomite cements of septarian cracks and veins at Mal Pass site.

Figure 12. $\delta^{18}O$ versus $\delta^{13}C$ cross plot for dolomite at Mal Pass site. Circles: concretion body; Squares: septarian cracks filling dolomite. Values relative to VPDB standard.

Figure 13. The Agnelli Fm. (A) Transmitted light and (B) crossed polars photomicrographs of a chert nodule/host limestone boundary. Echinoderm fragments are clearly recognizable in the

limestone. (C) Cathodoluminescence image of sponge spicules replaced by zoned non- to brightly luminescent calcite spar.

Figure 14. Schematic sketches, not to scale, representing the fluid pathways within the pre- to syn-rift rocks in the Adriatic distal margin at Middle Jurassic time and formation of siliceous septarian concretions (A). The dashed line indicates the location of a mass gravity flow involving concretions that are then included as reworked clasts in coarse turbidite beds of the Saluver Fm. (B).

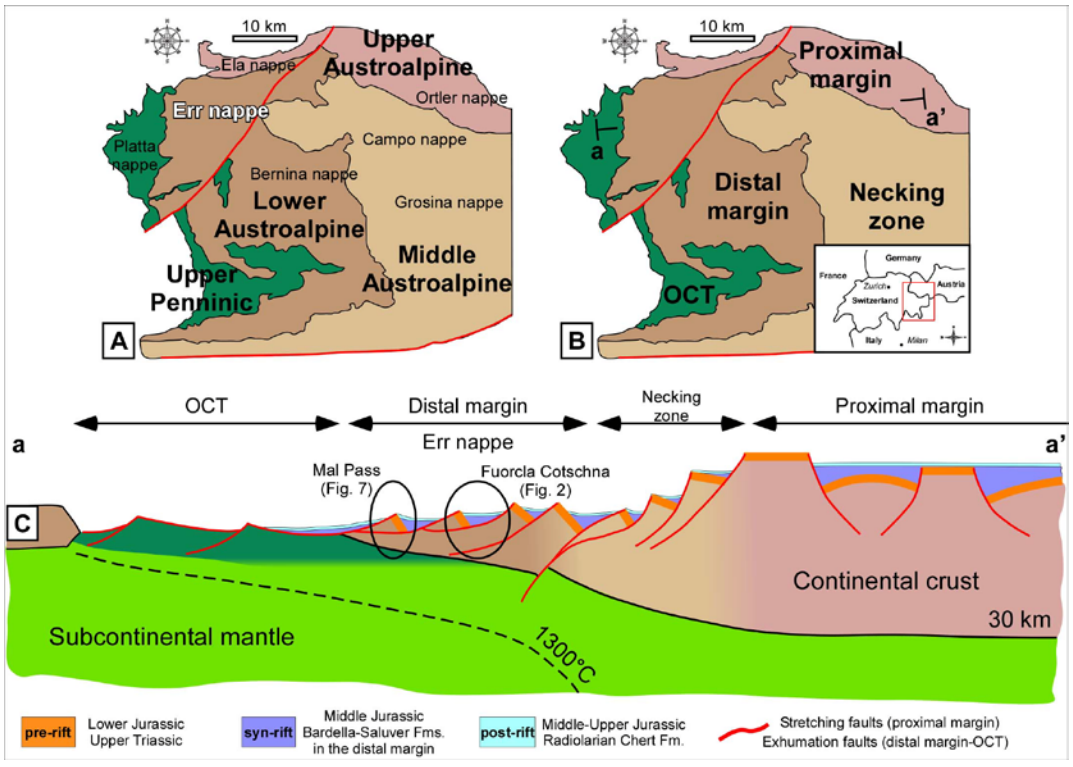

Fig. 1

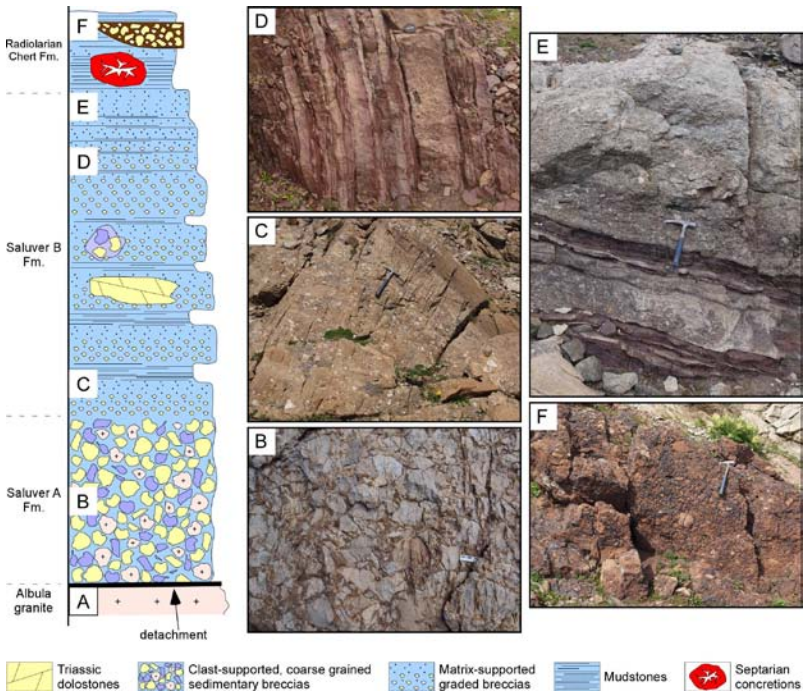
Radiolarian Chert Fm.
Saluver B Fm.
Saluver A Fm.
Albula granite
detachment
Triassic dolostones
Clast-supported, coarse grained sedimentary breccias
Matrix-supported graded breccias
Mudstones
Septarian concretions

Fig. 2

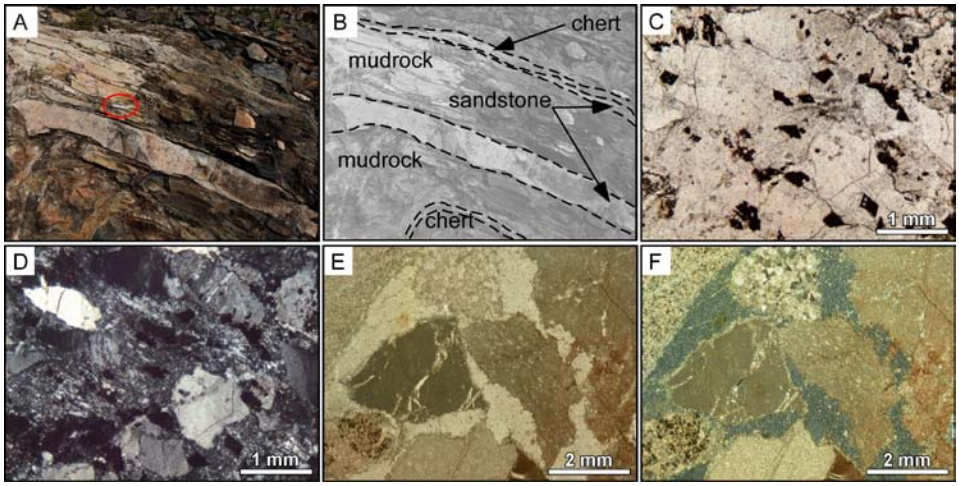
chert
mudrock
sandstone
mudrock
chert
1 mm
1 mm
2 mm
2 mm

Fig. 3

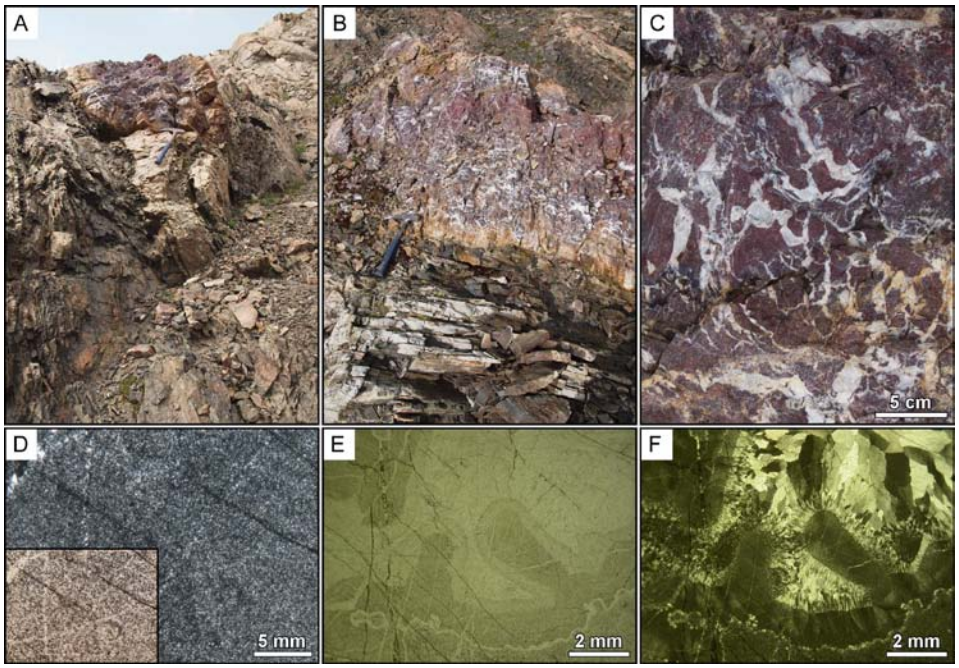

Fig. 4

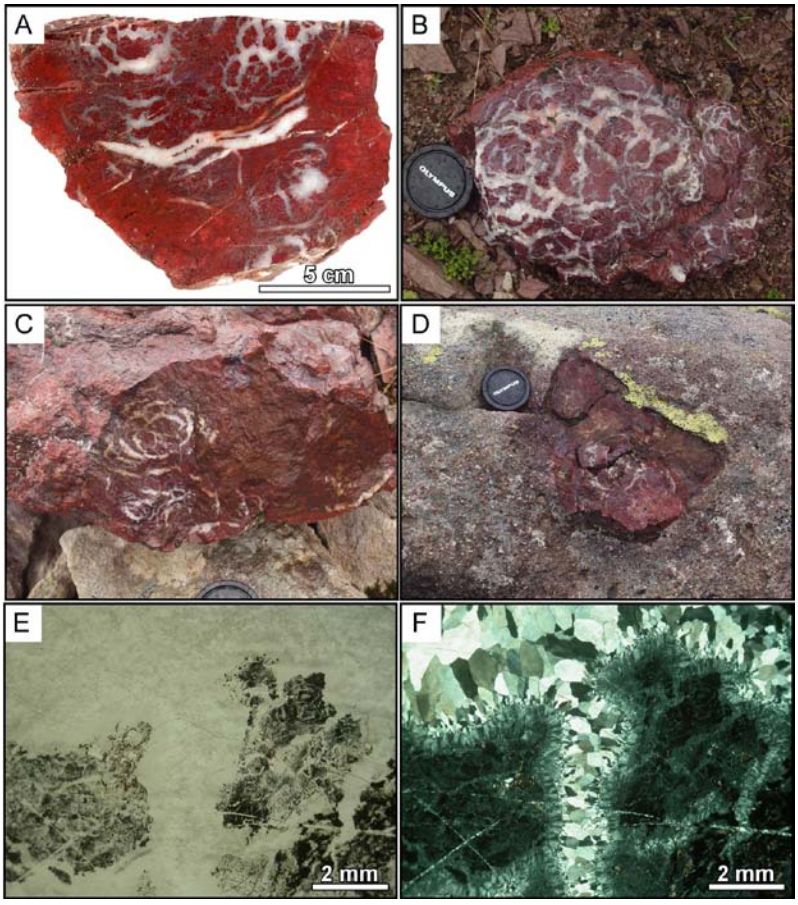

Fig. 5

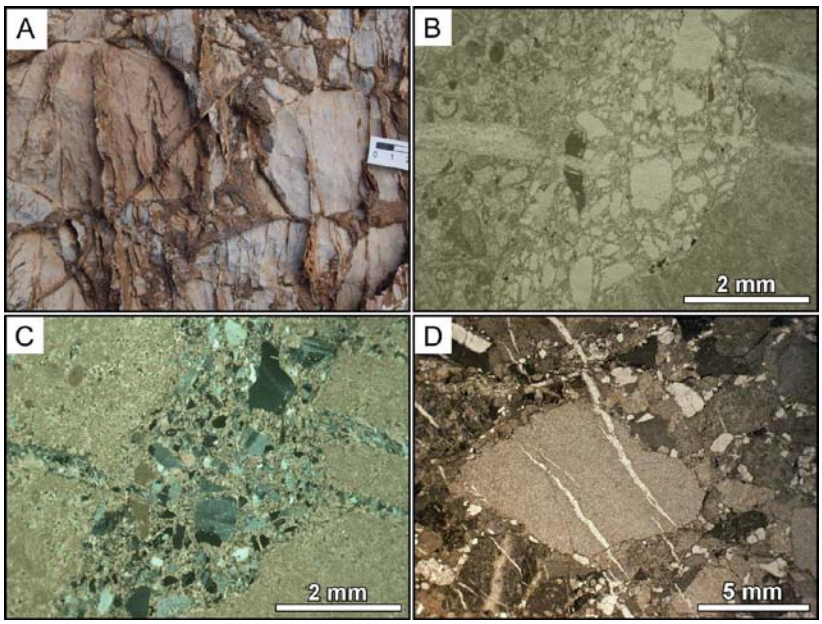

Fig. 6

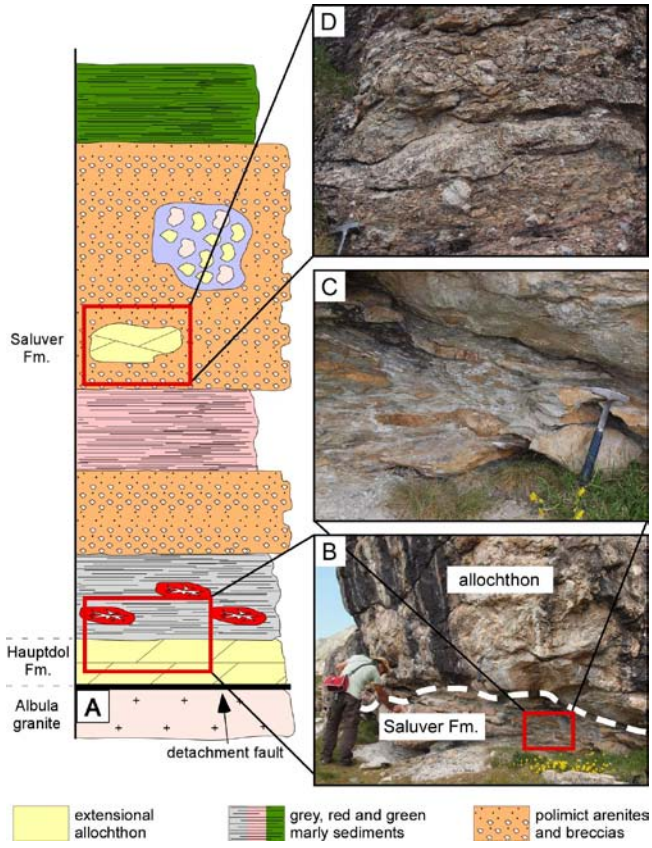
D
C
B
A
Saluver Fm.
Hauptdol Fm.
Albula granite
allochthon
Saluver Fm.
detachment fault
extensional allochthon
grey, red and green marly sediments
polimict arenites and breccias

Fig. 7

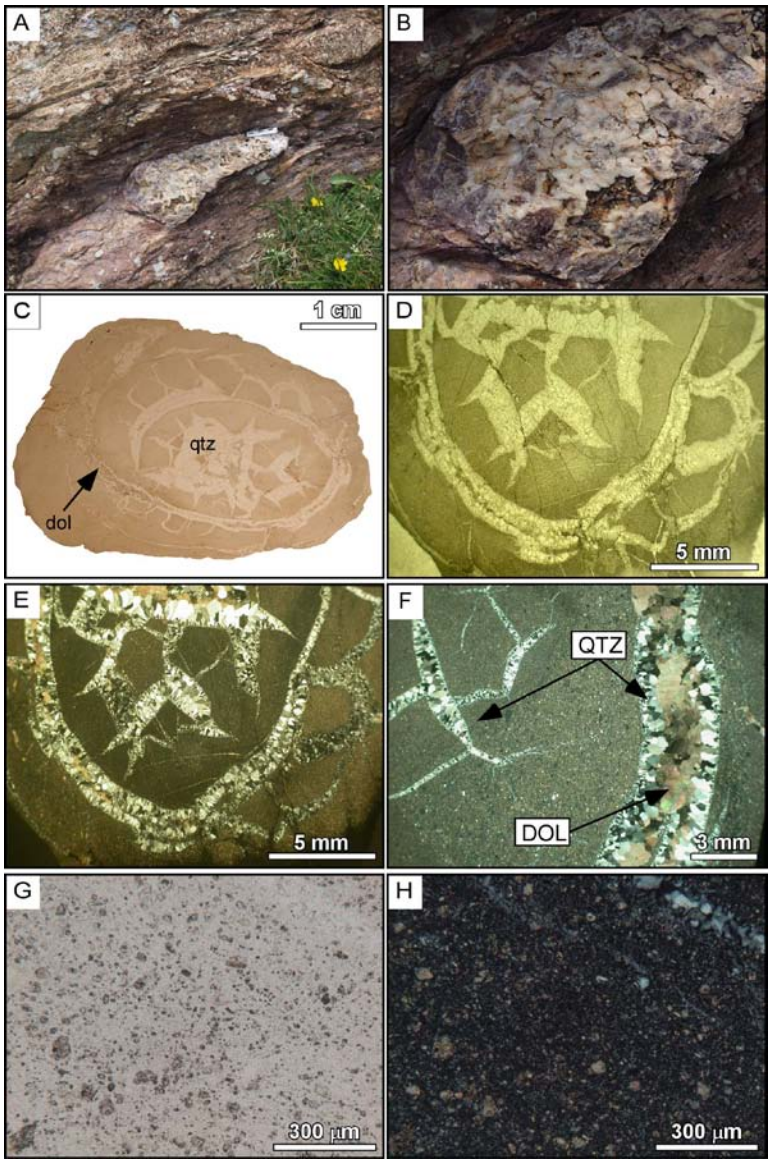

Fig. 8

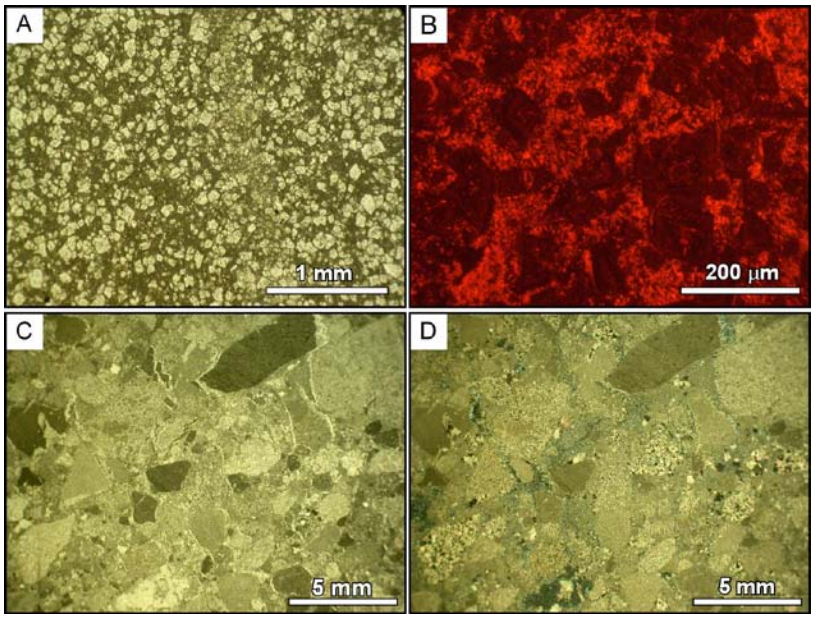

Fig. 9

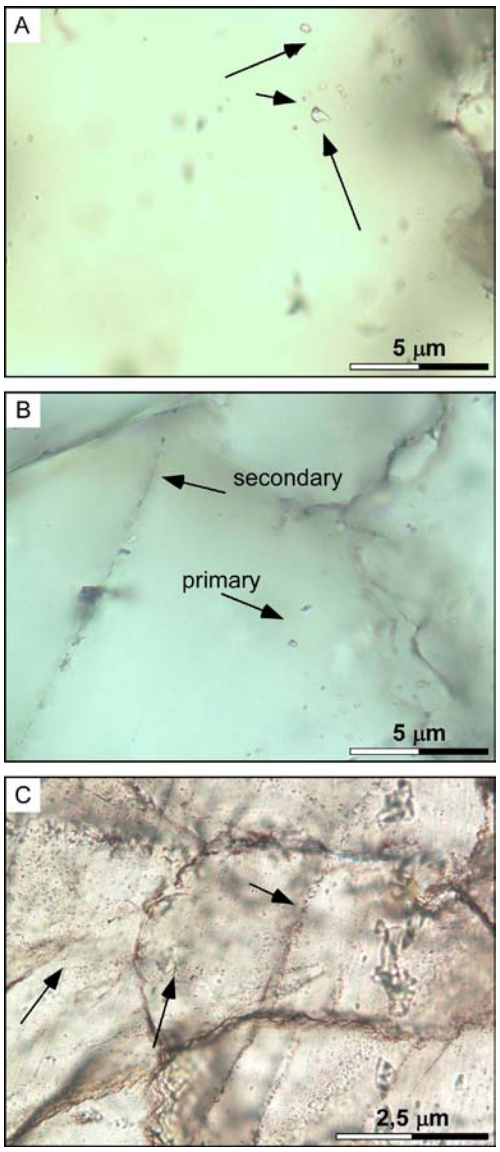

Fig. 10

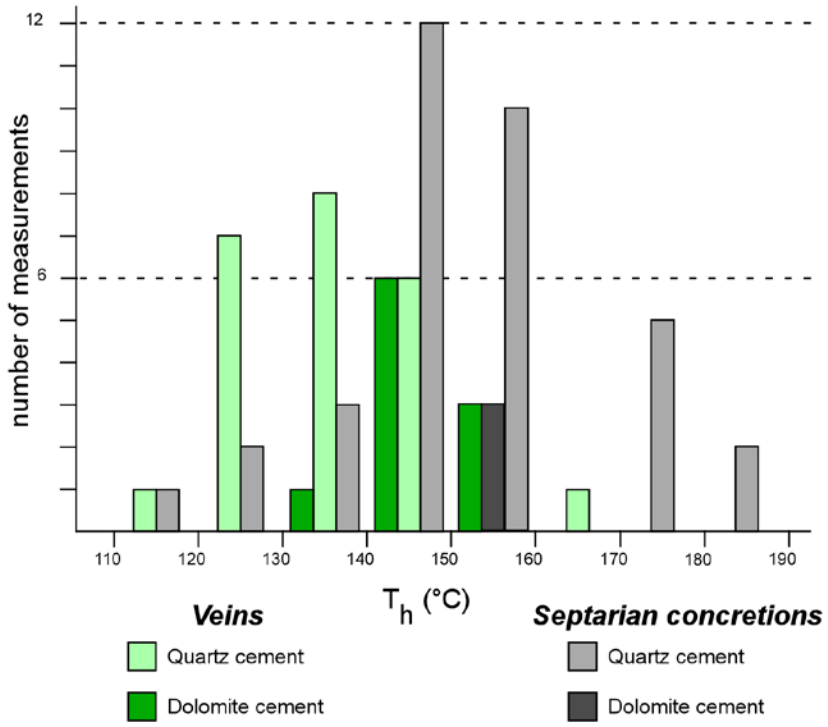
12
6
number of measurements
110
120
130
140
150
160
170
180
190
T h (°C)
Veins
Septarian concretions
Quartz cement
Dolomite cement
Quartz cement
Dolomite cement

Fig. 11

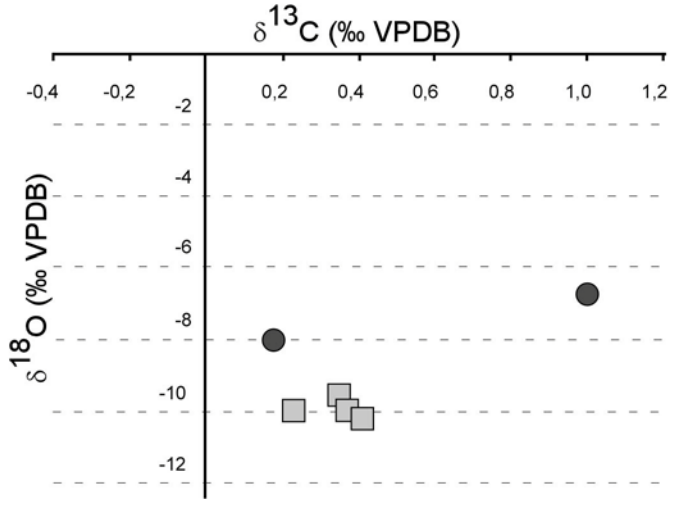
δ13C (‰ VPDB)
-0,4
-0,2
0,2
0,4
0,6
0,8
1,0
1,2
-2
-4
-6
-8
-10
-12
δ18O (‰ VPDB)

Fig. 12

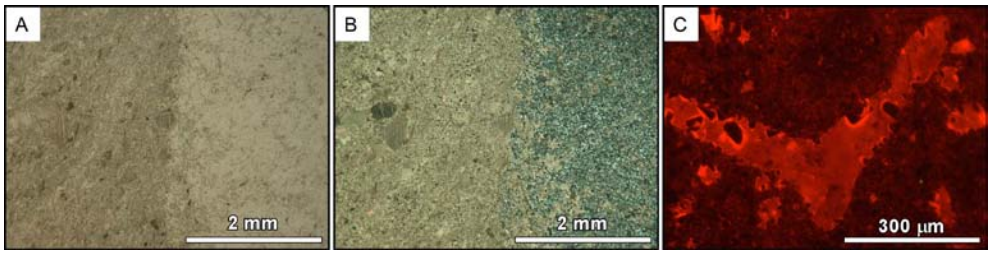
A
2 mm
B
2 mm
C
300 µm

Fig. 13

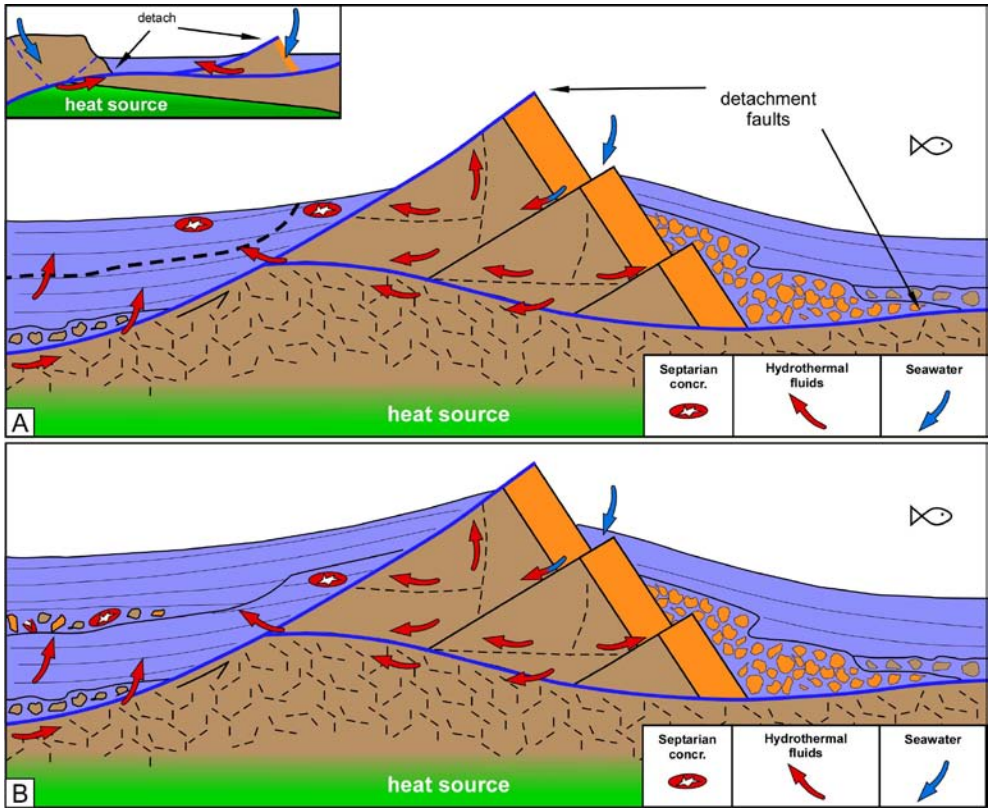
detach
heat source
detachment
faults
Septarian
concr.
Hydrothermal
fluids
Seawater
heat source
A
Septarian
concr.
Hydrothermal
fluids
Seawater
heat source
B

Fig. 14